Hindawi Publishing Corporation
International Journal of Photochemistry
Volume 2014, Article ID 721216, 8 pages
http://dx.doi.org/10.1155/2014/721216

Research Article

Effect of the Amount of Water in the Synthesis of B-TiO_2: Orange II Photodegradation

M. May-Lozano, G. M. Ramos-Reyes, R. López-Medina, S. A. Martínez-Delgadillo, J. Flores-Moreno, and I. Hernández-Pérez

Departamento de Ciencias Básicas, Universidad Autónoma Metropolitana-Azcapotzalco, Avenida San Pablo 180, Colonia Reynosa Tamaulipas, 02200 México, DF, Mexico

Correspondence should be addressed to M. May-Lozano; mml@correo.azc.uam.mx

Received 28 May 2014; Revised 10 August 2014; Accepted 11 August 2014; Published 28 August 2014

Academic Editor: Shinya Maenosono

A series of boron-doped TiO_2 photocatalysts (2% B-TiO_2) with different water/alkoxide molar ratio were synthesized by conventional sol-gel method. The prepared samples were characterized by BET measurement, X-ray diffraction (XRD), Fourier transform infrared spectroscopy (FTIRS), and diffuse-reflectance UV-vis. The phase anatase was present, but unexpectedly a small amount of rutile phase was formed with low and excess water in the synthesis. Additionally it has been observed that the increase in the molar ratio of water significantly increases the values of band gap energy and the specific surface area. Results showed that degradation of Orange II azo dye increases with surface area, particle size, boron, and water content in photocatalysis. The boron species were introduced in the tricoordinated form.

1. Introduction

Current emission of pollutants from textile industry to different bodies of water is a serious problem, not only since this industry uses large volumes of water, but also because most of these dyes are resistant to the conventional wastewater treatment processes. Different emerging technologies have been tested to try to solve this problem; among them, the advanced oxidation processes such as heterogeneous photocatalysis employing TiO_2 have demonstrated to be the most viable alternative to eliminate several organic contaminants [1, 2]. On the other hand titanium dioxide (TiO_2) has attracted growing scientific interest due to its good chemical and photochemical stability, nontoxicity, availability, low price, or ease of synthesis. However the structural, electronic, and photocatalytic properties of TiO_2 depend on the method of synthesis, while the size, morphology, and microstructure of crystals can be controlled and modified during hydrolysis and condensation steps [2–4]; that is, the water content changes the rate of hydrolysis. In order to improve its photocatalytic activity and shift its absorption band towards the visible region, several attempts have been also made to narrow the band gap energy by doping with various metals ions [5, 6], where it is suggested that the incorporation of metal to TiO_2 structure modifies both the charge carriers recombination rate and the interfacial electron-transfer rate, as well as the generation of recombination sites or the band gap energy, depending on where these ions are located in the TiO_2 structure. On the other hand the doping of TiO_2 with non metals atoms such as carbon, nitrogen or boron atoms [7–12] have shown a higher photoactivity performance under visible light irradiation. The photoreactivity of doped TiO_2 is a complex function of the dopant concentration, the energy level, the *d* electronic configuration, the distribution of dopants, the electron donor concentration, and the light intensity [5]. Photocatalysis involves the absorption of photons by a molecule or the substrate to produce reactive electronically excited states and the photocatalysis process by TiO_2 is the generation of electron-hole pairs [5, 13]. Metal and nonmetal dopants influence the photoreactivity of TiO_2 by acting as electron and hole traps and by altering the e^-/h^+ pair recombination [13].

The boron (nonmetal) doping to the TiO_2 has been studied in the literature and the doping content as well

Table 1: H_2O content, specific surface area, and the average pore size of samples.

Photocatalyst	% boron	H_2O/alkoxide	Average pore diameter (nm)	BET surface area (m^2/g)
TiO_2-4	0	4	30.1	27.7
$BTiO_2$-0.5	2.5	0.5	15.5	3.1
$BTiO_2$-1	2.5	1	7.3	17.0
$BTiO_2$-4	2.5	4	7.1	20.8
$BTiO_2$-8	2.5	8	12.7	46.0
$BTiO_2$-16	2.5	16	24.9	29.1

as the chemical state of boron element affects much the photocatalytic activity of the photocatalyst [14–17]. Likewise, it has been found that the selectivity was improved in degradation of pollutants when boron was used to dope the TiO_2 in photocatalytic reactions.

In this research, the effect of the amount of water on the synthesis of boron-doped TiO_2 photocatalyst by sol-gel method was studied. Few studies are on the water content during the synthesis of TiO_2 [18, 19]. Some authors have found that the higher photoactivity was shown by materials with boron content around 2-3 wt% of boron [15, 20, 21]. Moreover, the boron is a nonmetal that has been less studied doping TiO_2 and the corresponding literature is controversial [17]. According to this, the aim of this study is to find a relationship between the molar ratio water/alkoxide with structural, textural, and photoactivity properties of B-TiO_2 system and to determine the type of boron species present in this system, which can be responsible for the photoactivity.

The B-TiO_2 samples were characterized by X-ray diffraction (XRD), Brunauer-Emmett-Teller (BET) measurement, and diffuse-reflectance UV-vis spectroscopy. The study of the degradation of Orange II was carried out by UV-visible spectrophotometer.

2. Experimental

2.1. 2% B-TiO_2 Oxide Preparation. A series of 2% B-TiO_2 materials and pure TiO_2 (as reference) were prepared by sol-gel method. The B-TiO_2 catalysts were prepared to obtain a content of 2% of boron. During solids synthesis the amount of water was modified (molar ratio water/alkoxide = 0.5, 1, 4, 8, and 16) and the catalysts with different water contents were called $BTiO_2$-X, in which X indicates the amount of water used in the synthesis (see Table 1). The TiO_2 used as reference was called TiO_2-4 (water/alkoxide = 4). Butanol and titanium isopropoxide were used in a molar ratio alcohol/alkoxide = 10. In a three-neck flask butanol, titanium isopropoxide, and boric acid were mixed at room temperature and an appropriate amount of deionized water was added dropwise into the solution. The X = H_2O/alkoxide molar ratios used were 0.5, 1, 4, 8, or 16 and the solution was kept under stirring for 2 hours. Then, the samples were dried at 100°C in oven for 2 days and finally calcined in muffle furnace at 450°C using a heating rate of 5°C/min for 3 h. Pure TiO_2 was synthesized in the same manner as the sample with water/alkoxide = 4 content, but boric acid was not added to this material during the synthesis.

2.2. Catalysts Characterization. The structural characterization of solids was carried out by powder XRD using a Philips X'Pert diffractometer, operating in 2θ mode; samples were analyzed in the range of 20 to 80, 2θ degrees using a Cu tube Kaα radiation (35 kV, 25 mA) at $2^\circ\,s^{-1}$ scan rate, and wavelength $\lambda = 0.15405$ nm. The surface areas were calculated by BET method and the pore volume was determined by the Barrett-Joiner-Halenda (BJH) method. The study was obtained on a BELSORP-max nitrogen adsorption apparatus at a temperature around 73 K. The sample was treated at 298°C before measurement. The optical properties of materials were determined using an UV-vis (Varian Cary 1 double-beam) spectrophotometer operating in the diffuse reflectance mode. The FT-IR spectroscopic measurements were carried out using a Nicolet Magna spectrophotometer and the spectra were recorded using a KBr wafer technique.

2.3. Degradation of Orange II

2.3.1. Adsorption Experiments. Degradation of Orange II dye was studied by catalytic reaction. The tests were carried out in a stirred batch reactor; it is placed inside an aluminum foil box at room temperature. In a reactor with 25 mL of Orange II solution 0.3 g of the catalyst was added, with an initial concentration of 10 mg/L of dye. The pH was monitored as a function of time and remained close to 7. Reaction monitoring is performed by a Varian Cary 1 UV-vis Spectrophotometer, which determined the amount of degraded dye and the study was carried out for 2 hours. In the quantification, the absorbance was analyzed with the wavelength of 485 nm. Likewise, in all cases, also studies were conducted without catalyst and the dye was not degraded.

2.3.2. Photocatalytic Degradation of Orange II. The same conditions of the catalytic reaction were used, but in this case a UV lamp was placed at the top of the reactor. The reactor was irradiated by the UV light at wavelength 365 nm (lamp power 5 W). Likewise, tests were conducted without catalyst and the dye was not degraded. The pH of solution was 7 and no significant modification of the pH was observed during the experiments. Figure 1 shows the photocatalytic reaction system, which is illustrated as the degradation is carried out

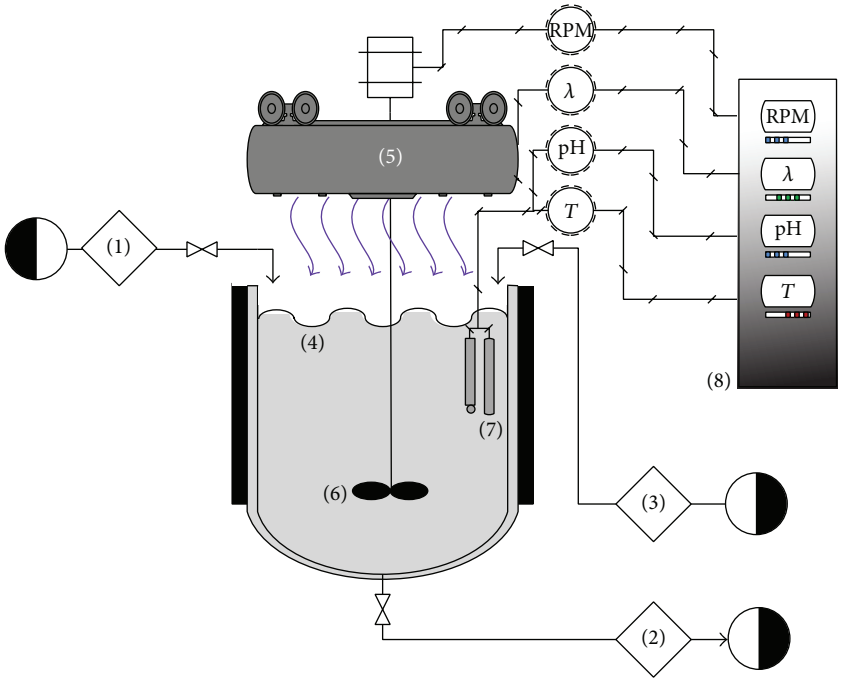

Figure 1: Photocatalytic reactor system: (1) dye solution, (2) UV-vis sampling, (3) sample return, (4) batch reactor, (5) lamp, (6) stirrer, (7) sensors, and (8) monitor.

using a UV lamp. The UV lamp is placed above the reactor and the reaction was maintained under moderate stirring.

3. Results and Discussion

3.1. Textural Analysis. Figure 2 and Table 1 present the textural properties of $BTiO_2$-X samples; these results show that the average pore diameter of $BTiO_2$-X samples was increased with increasing the water content in the synthesis, and a similar behavior occurs with the specific surface area and the pore volume, except the sample with a molar ratio of 16% (Figure 2). The surface area of the TiO_2 without boron (TiO_2-4) is larger than the sample containing boron ($BTiO_2$-4, see Table 1). The decrease in the specific areas and the pore diameters due to the presence of boron is known in the literature [22]. Štengl et al. [22] found that the specific surface area from the BET had tendency to decrease with increasing content of boron and the pore size distribution indicated conversion from micropores to mesopores with increasing amount of boron, but samples with the highest content of boron became microporous. The size of the pore diameter is different between the sample without boron (TiO_2-4, 30.1 nm) and the sample with boron ($BTiO_2$-4, 7.1 nm); there is a decrease, which can be attributed to the particle size (see XRD section). There is a strong dependence between the dimensions of the particles and the pore diameters [23]; smaller particles lead to small pores. Figure 2 shows the pore volume of $BTiO_2$-X samples; the pore volume increases with higher water concentrations in the synthesis.

The particles with different size have different surface area and pore volume [2, 23]. A greater amount of water during the synthesis leads to increase of hydrolysis and condensation allowing an increase in the formation of Ti–O–B and Ti–O–Ti groups [16]. The changes in surface area and pore volume of $BTiO_2$-X samples are related to the size of the particles or the largest number of particles formed. The specific surface area and anatase phase are important in the photocatalysis of TiO_2 [4]. Therefore, the greater specific surface area for the B-TiO_2 with high water concentration in the synthesis is due to the formation of larger pore volume between aggregated particles (Figure 2).

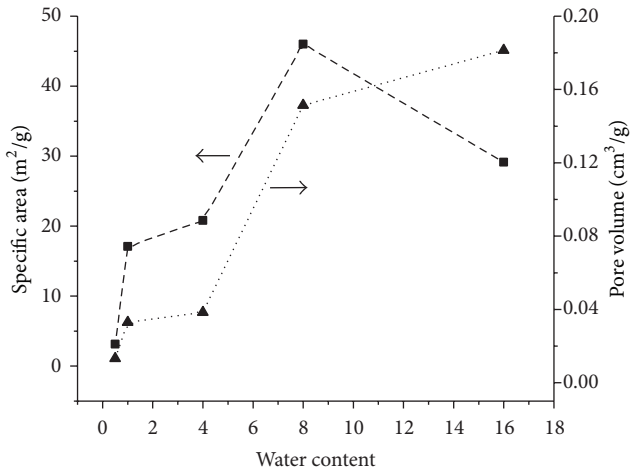

Figure 2: The BET surface areas and pore volume of $BTiO_2$-X samples.

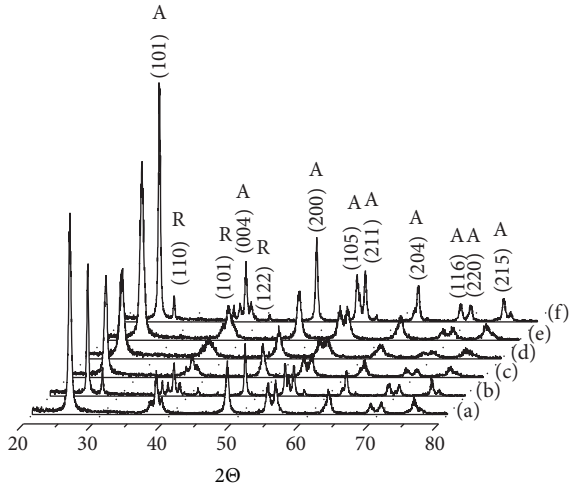

Figure 3: XRD patterns of (a) TiO_2-4, (b) $BTiO_2$-0.5, (c) $BTiO_2$-1, (d) $BTiO_2$-4, (e) $BTiO_2$-8, and (f) $BTiO_2$-16; A and R represent anatase and rutile, respectively.

3.2. XRD. Figure 3 shows the XRD patterns of the solids. In the case of TiO_2-4 only well-defined diffractions of anatase phase (JPCDS 21-1272) can be seen in the pattern at $2\theta = 25.4^\circ$ (101), 38.0° (004), 48.2° (200), 54.1° (105), 55.1° (211), 62.8° (204), 68.9° (116), 70.3° (220), and 75.2° (205); the number in the parenthesis indicates the hkl values [24]. The XRD powder patterns of the week rutile phase (JPCDS 21-1276) at $2\theta = 27.4^\circ$ (110), 36.1° (101), and 41.2° (122) appeared in $BTiO_2$-0.5 and $BTiO_2$-16 with different ratio of water/alkoxide (Figure 3). The weight fractions were calculated from the relative intensities of the strongest peaks for anatase (101) and rutile (110). The average crystal size is presented in Table 2 calculated from the strongest diffraction peak at $2\theta = 25.4^\circ$ in the (101) reflection using the Scherrer equation:

$$d = \frac{k\lambda}{\beta \cos\theta}, \quad (1)$$

where λ is the wavelength of the Cu Kα radiation used (1.542 Å), β is the full width at half maximum of the diffraction angle considered, k is the shape factor (0.89), and θ is the angle of diffraction.

The relative intensity of the peaks of $BTiO_2$-X samples is weakened and broadened compared with those of the TiO_2 [25] (Figure 3). No crystalline phase assigned to B_2O_3 could be found in any B-TiO_2 catalysts because the concentration of B_2O_3 is so low or the boron species in all samples are highly dispersed on TiO_2 support [26]. As it is well known, sol-gel method is an easy route to obtain high purity nanosized TiO_2 at mild synthesis conditions. It has been well established that the photoactivity of TiO_2 is correlated with its crystallinity and particle size. It can be clearly observed that the crystallinity of these $BTiO_2$-X samples is different. Table 2 shows that the $BTiO_2$-4 has the smallest particle size (11 nm) which indicated that the water in the synthesis would generate a distortion in the crystalline structure. These results indicate that the boron acted as an inhibitor for the growth of the anatase nanoparticles, because pure TiO_2 has larger particle size (TiO_2-4 = 14 nm).

The results of XRD show that water content has the greatest effect on the particle size and crystal phase of B-TiO_2. The obtained XRD patterns showed that with the excess amount of water ($BTiO_2$-16) used in the synthesis the particle size increased, and peaks became more evident and could result in more –OH groups on the surface of nanoparticles. Increasing the water content, the hydrolysis occurs more quickly and much more Ti–O–Ti, Ti–O–B, or Ti–O–H groups are produced. The intensity of the XRD peaks increases with increasing water content in the synthesis, and then this indicates an increase in the crystal phase (anatase).

In similar synthesis conditions regularly pure anatase phase is obtained, but unexpectedly rutile phase was formed. This study found that the rutile phase was present when the particle size is large ($BTiO_2$-0.5 and $BTiO_2$-16, see Table 2). This suggests that low and excessive water additive caused a phase transition for the synthesized $BTiO_2$-16 (Figure 3). Results are consistent with studies where rutile is obtained by thermal methods or boron doped [16, 26, 27], where the rutile has a significant increase when there is an increase in the crystal size (Table 2). The formation of rutile at low water concentration synthesis ($BTiO_2$-0.5) could be because few groups Ti–O–Ti are formed during the initial synthesis; possibly the bonds Ti–O–Ti are formed during drying or calcination. Moreover, the formation of rutile with excess water in the synthesis ($BTiO_2$-16) is explained by a structural rearrangement of the catalyst. The anatase to rutile rearrangement involves breaking of two of the six Ti–O bonds in anatase [13]. During the temperature treatment the water excess causes the Ti–O–Ti network to weaken and this facilitates the Ti–O bond breaking and a consequent structural rearrangement to more stable rutile phase. The water in excess is lost by evaporation of solid, leaving behind oxygen vacancies, which accelerates the Ti–O bond breaking and crystallite growth. In this case, boron is certainly helping in the process of rutile formation.

With low water molar ratios (0.5 to 4) the particle size decreases, whereas it increases with a water excess (8–16) (Table 2). The lattice parameters a and c are affected with possible transitions of the crystal phases (Table 2). Sample $BTiO_2$-4 prepared with a stoichiometric ratio of water ($4H_2O$: 1 alkoxide) is slightly distorted as indicated by its parameter c (9.42 Å) which is the closest to the data reported for the anatase (c = 9.51 Å) [13].

3.3. Bandgap Determination. UV-vis DRS spectra of $BTiO_2$-X photocatalysts are shown in Figure 4. The estimates band gap (E_g) was obtained from extrapolation of the linear region of the Kubelka-Munk transformation of the UV-vis absorption spectra ($F(R) = 0$), as shown in Figure 4.

A relevant property to the photocatalytic activity of a semiconductor is its energy band configuration, the photons with energy equal to or higher than the band gap (Eg) promote formation of electron-hole pairs and the redox capabilities of excited-state electrons and holes. The band gaps of the $BTiO_2$-X samples are presented in Table 2. The band

Table 2: Lattice parameters (Å), crystal size (nm), and band gap (eV) of the photocatalysts. Physical properties derived based on d_{101} and the tetragonal unit cell to TiO_2 anatase.

Photocatalyst	FWHM[a]	Lattice parameters (Å)	E_g (eV)	d (nm)	Composition[b]
TiO_2-4	0.602	$a = 3.79$; $c = 9.42$	3.16	14	(A) 100%
$BTiO_2$-0.5	0.272	$a = 3.78$; $c = 9.37$ $a = 4.58$; $c = 2.98$	2.96	30	(A) 84% (R) 16%
$BTiO_2$-1	0.544	$a = 3.79$; $c = 9.38$	3.00	15	(A) 100%
$BTiO_2$-4	0.766	$a = 3.80$; $c = 9.42$	3.14	11	(A) 100%
$BTiO_2$-8	0.608	$a = 3.77$; $c = 9.37$	3.16	14	(A) 100%
$BTiO_2$-16	0.337	$a = 3.78$; $c = 9.39$ $a = 4.56$; $c = 2.98$	3.00	24	(A) 89% (R) 11%

[a]Full width at half maximum (FWHM).
[b]Anatase (A) and rutile (R).

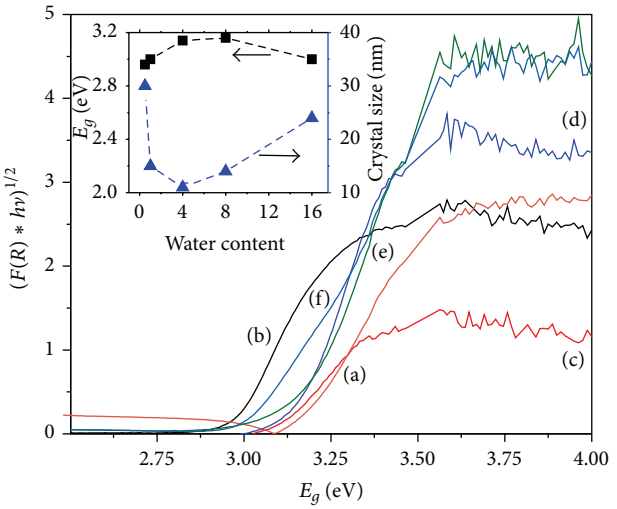

Figure 4: $(F(R) * hv)^{1/2}$ versus photon energy (E_g); (a) TiO_2-4, (b) $BTiO_2$-0.5, (c) $BTiO_2$-1, (d) $BTiO_2$-4, (e) $BTiO_2$-8, and (f) $BTiO_2$-16.

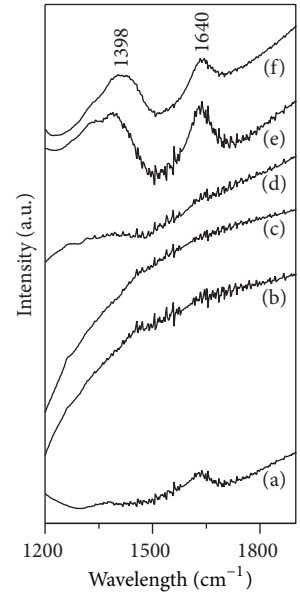

Figure 5: FT-IR spectra of (a) TiO_2-4, (b) $BTiO_2$-0.5, (c) $BTiO_2$-1, (d) $BTiO_2$-4, (e) $BTiO_2$-8, and (f) $BTiO_2$-16.

gap energies (E_g values) suggest a decrease in the intrinsic band gap of B doped TiO_2 [28]. Thus boron incorporation into TiO_2 lattice alters the electronic structure leading to the appearance of intermediate energy level [29, 30]. The band gap energy of $BTiO_2$-X catalysts is lower than the pure TiO_2 (3.16 eV, ca 380 nm) making it hardly absorbed in visible light region [31–33]. When the TiO_2 surface was modified with the boron ions, adsorption in the visible region increased, and therefore the number of photogenerated electrons and holes increased [34]. With the increase of water in the synthesis the band gap increases (Figure 4). However, when there is an excess of water ($BTiO_2$-16) the band gap decreases probably due to the formation of large particle size. Figure 4 (top left) shows a marked inverse relationship between particle size and E_g; it means that particles with larger sizes lead to lower energies, which are in good agreement with the quantum confinement effect.

3.4. FT-IR of B-TiO_2. Figure 5 shows FT-IR spectra of $BTiO_2$-X photocatalysts. For samples, the bands at 1398 cm^{-1} can be ascribed to the vibration of tricoordinated interstitial boron (in the form of B^{3+}) [20, 27] and the band at 1640 cm^{-1} is assigned to the stretching of hydroxyl groups and the bending vibration of H_2O adsorbed on the surface of the samples. In the IR spectra of the samples, another small peak appears at 1280 cm^{-1} which can be ascribed to the stretching vibration of the B–O bonds of boroxol rings [27].

Results reveal that boron is introduced into the titania framework in the form of B–O–Ti bond, corresponding to tricoordinated interstitial boron. The results indicate that the boron species are introduced in the tricoordinated form mainly with high amounts of water used in the synthesis. This indicates that boron is more easily trapped into the titania framework when hydrolysis is favored. The peak at 1640 cm^{-1} which is related to vibration of water also increases, because larger amount of water in the synthesis results in the formation of higher content of hydroxyl groups in the samples.

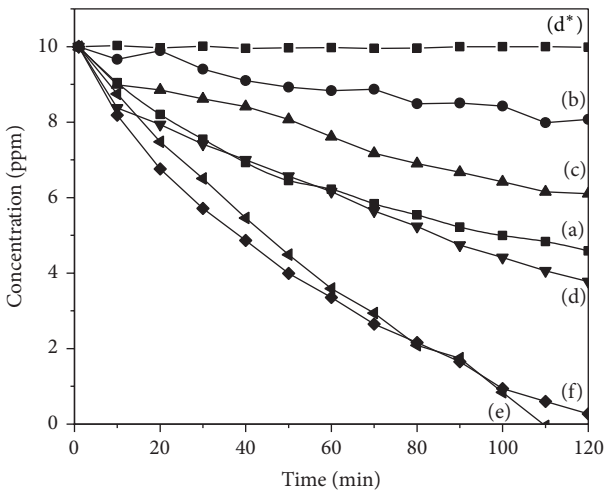

Figure 6: Photocatalytic reactions of the samples, ■ (a) TiO_2-4, ● (b) $BTiO_2$-0.5, ▲ (c) $BTiO_2$-1, ▼ (d) $BTiO_2$-4, ◄ (e) $BTiO_2$-8, ► (f) $BTiO_2$-16, and ■ (d*) $BTiO_2$-4 catalytic degradation without lamp.

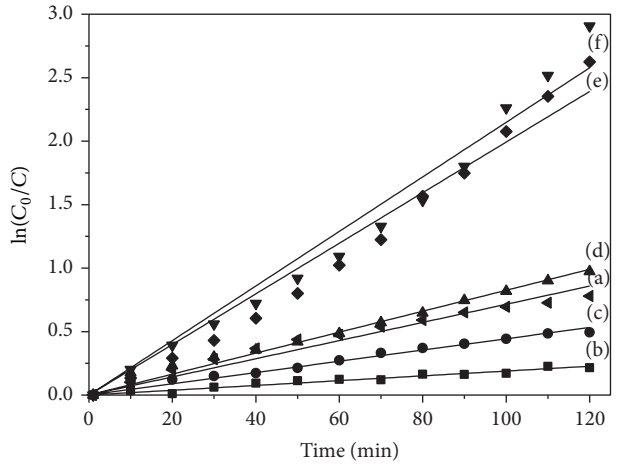

Figure 7: Kinetics of Orange II photodegradation; ■ (a) TiO_2-4, ● (b) $BTiO_2$-0.5, ▲ (c) $BTiO_2$-1, ► (d) $BTiO_2$-4, ◄ (e) $BTiO_2$-8, and ▼ (f) $BTiO_2$-16.

3.5. Adsorption Study. The catalytic activity of the $BTiO_2$-X catalysts for the degradation of Orange II was evaluated without UV irradiation. In all catalysts, the Orange II concentration decreases slightly, indicating that the degradation of Orange II is very limited. The presence of the catalyst without light does not allow an efficient degradation of the dye. In the catalysts, the concentration of water during the synthesis of $BTiO_2$-X was not a critical factor in the degradation of the dye. The low activity is present in all of the catalysts with or without boron. Figure 6(d*) displays the Orange II concentration as a function of the reaction time of the $BTiO_2$-4 catalyst without visible light. The activity of other catalysts ($BTiO_2$-X and TiO_2-4) was very similar.

3.6. Photocatalytic Test. The photocatalytic activity of the B-TiO_2 catalyst for the degradation of Orange II was evaluated with a reactor irradiated by UV light at wavelength 365 nm. Figure 6 displays the Orange II concentration as a function of the reaction time. It can be seen that increasing the amount of water in the synthesis promotes an increase in the Orange dye degradation. An exception is the catalyst $BTiO_2$-16, where this catalyst with more water shows different behavior (Figure 6(f)). The $BTiO_2$-8 (e) after 2 hours of reaction showed a slightly higher activity than $BTiO_2$-16. Also, Figure 6 shows a comparison between the $BTiO_2$-4 (d) and TiO_2 (TiO_2-4 (a)) photocatalysts, which were synthesized with the same amount of water. $BTiO_2$-4 photocatalyst containing boron has greater activity than TiO_2-4, which is the catalyst without boron. The above results confirm that the photocatalysis is favored with the boron content and the increase of water in the synthesis. The tricoordinated interstitial boron could also play an important role in the catalytic degradation (see Figure 5). Heterogeneous photocatalysis followed the first order kinetics for Orange II degradation (Figure 7). Kinetics of Orange II photodegradation shows that the photocatalytic activity increases when the molar ratio of water increases from 0.5 to 16. According to the overall results of our investigation, we have found that a high specific surface area and the presence of the anatase phase of TiO_2 are indispensable in the photodegradation of Orange II but are not the only determinant factors; on the contrary, it is important to note that the photocatalytic behavior of B-TiO_2 system can be explained more appropriately, not only considering the values of E_g, but also taking into consideration the type of electronic states induced by the addition of boron. Additionally, it is important to consider that the incorporation of nonmetallic dopants, such as boron, occupying interstitial sites in the anatase TiO_2 structure, can generate reduced Ti^{3+} species, which can act as traps for electrons or holes. As expected, several parameters are related to the photoactivity of the B-TiO_2 nanoparticles, so additional characterization studies are in progress in our laboratory.

4. Conclusions

BET results indicated that specific surface area increased with increasing water content in the synthesis of $BTiO_2$-X and the powders calcined at 450°C had anatase phase. However, the samples with low and high ratio of water have some content of rutile. The results showed that large amounts of water increase the crystal size and excessive water in the preparation causes a phase transition from anatase to rutile. Increasing water content in the synthesis increases the crystal phase (anatase) and the band gap energies. With the increase of water in the synthesis the band gap increases and the band gap decreases due to the presence of large particle size. The photocatalytic activity of $BTiO_2$-X powders for the degradation of Orange II increased with increasing water in the synthesis. It is noteworthy that the specific surface area and particle size of $BTiO_2$-X nanoparticles were dominant factors controlling the photocatalytic activity. As reported in recent times, the results indicate that the boron

content improves photocatalytic activity. It is also necessary to mention that boron is more easily trapped inside the TiO_2 when there is more water in the synthesis (in the form of B^{3+}).

Conflict of Interests

The authors declare that there is no conflict of interests regarding the publication of this paper.

Acknowledgment

Ricardo López acknowledges the support provided by CONACYT (206771) to perform a postdoctoral fellowship at UAM-A, as well as support for the project CONACYT (CB-201169786-Y).

References

[1] N. Xu, Z. Shi, Y. Fan, J. Dong, J. Shi, and M. Z. C. Hu, "Effects of particle size of TiO_2 on photocatalytic degradation of methylene blue in aqueous suspensions," *Industrial and Engineering Chemistry Research*, vol. 38, no. 2, pp. 373–379, 1999.

[2] K. Natarajan, T. S. Natarajan, H. C. Bajaj, and R. J. Tayade, "Photocatalytic reactor based on UV-LED/TiO_2 coated quartz tube for degradation of dyes," *Chemical Engineering Journal*, vol. 178, pp. 40–49, 2011.

[3] H. Lee, M. Choi, Y. Kye, M. An, and I. M. Lee, "Control of particle characteristics in the preparation of TiO_2 nano particles assisted by microwave," *Bulletin of the Korean Chemical Society*, vol. 33, no. 5, pp. 1699–1702, 2012.

[4] E. Kim, D. S. Kim, and B. Ahn, "Synthesis of Mesoporous TiO_2 and its application to photocatalytic activation of methylene blue and E. coli," *Bulletin of the Korean Chemical Society*, vol. 30, no. 1, pp. 193–198, 2009.

[5] R. J. Tayade, H. C. Bajaj, and R. V. Jasra, "Photocatalytic removal of organic contaminants from water exploiting tuned bandgap photocatalysts," *Desalination*, vol. 275, no. 1–3, pp. 160–165, 2011.

[6] R. J. Tayade, R. G. Kulkarni, and R. V. Jasra, "Transition metal ion impregnated mesoporous TiO_2 for photocatalytic degradation of organic contaminants in water," *Industrial and Engineering Chemistry Research*, vol. 45, no. 15, pp. 5231–5238, 2006.

[7] H. Irie, Y. Watanabe, and K. Hashimoto, "Carbon-doped anatase TiO_2 powders as a visible-light sensitive photocatalyst," *Chemistry Letters*, vol. 32, no. 8, pp. 772–773, 2003.

[8] S. Yang and L. Gao, "New method to prepare nitrogen-doped titanium dioxide and its photocatalytic activities irradiated by visible light," *Journal of the American Ceramic Society*, vol. 87, no. 9, pp. 1803–1805, 2004.

[9] H. Liu and L. Gao, "(Sulfur, nitrogen)-codoped rutile-titanium dioxide as a visible-light-activated photocatalyst," *Journal of the American Ceramic Society*, vol. 87, no. 8, pp. 1582–1584, 2004.

[10] S. U. M. Khan, M. Al-Shahry, and W. B. Ingler Jr., "Efficient photochemical water splitting by a chemically modified n-TiO_2," *Science*, vol. 297, no. 5590, pp. 2243–2245, 2002.

[11] T. Umebayashi, T. Yamaki, H. Itoh, and K. Asai, "Band gap narrowing of titanium dioxide by sulfur doping," *Applied Physics Letters*, vol. 81, no. 3, pp. 454–456, 2002.

[12] J. C. Yu, W. Ho, Z. Jiang, and L. Zhang, "Effects of F-doping on the photocatalytic activity and microstructures of nanocrystalline TiO_2 powders," *Chemistry of Materials*, vol. 14, no. 9, pp. 3808–3816, 2002.

[13] A. L. Linsebigler, G. Lu, and J. T. Yates Jr., "Photocatalysis on TiO_2 surfaces: principles, mechanisms, and selected results," *Chemical Reviews*, vol. 95, no. 3, pp. 735–758, 1995.

[14] A. C. Pierre, *Introduction to Sol-Gel Processing*, Kluwer Academic Publishers, 2002.

[15] E. Grabowska, A. Zaleska, J. W. Sobczak, M. Gazda, and J. Hupka, "Boron-doped TiO_2: characteristics and photoactivity under visible light," *Procedia Chemistry*, vol. 1, no. 2, pp. 1553–1559, 2009.

[16] D. Chen, D. Yang, Q. Wang, and Z. Jiang, "Effects of boron doping on photocatalytic activity and microstructure of titanium dioxide nanoparticles," *Industrial and Engineering Chemistry Research*, vol. 45, no. 12, pp. 4110–4116, 2006.

[17] W. Zhang, X. Li, G. Jia et al., "Preparation, characterization, and photocatalytic activity of boron and lanthanum co-doped TiO_2," *Catalysis Communications*, vol. 45, pp. 144–147, 2014.

[18] C. C. Wang and J. Y. Ying, "Sol-gel synthesis and hydrothermal processing of anatase and rutile titania nanocrystals," *Chemistry of Materials*, vol. 11, no. 11, pp. 3113–3120, 1999.

[19] X. Ding, Z. Qi, and Y. He, "Effect of hydrolysis water on the preparation of nano-crystalline titania powders via a sol-gel process," *Journal of Materials Science Letters*, vol. 14, no. 1, pp. 21–22, 1995.

[20] W. Zhang, B. Yang, and J. Chen, "Effects of calcination temperature on preparation of boron-doped TiO_2 by sol-gel method," *International Journal of Photoenergy*, vol. 2012, Article ID 528637, 8 pages, 2012.

[21] W. Zhang, X. Pei, B. Yang, and H. He, "Effects of boron content and calcination temperature on properties of B-TiO_2 photocatalyst prepared by solvothermal method," *Journal of Advanced Oxidation Technologies*, vol. 17, no. 1, pp. 66–72, 2014.

[22] V. Štengl, V. Houškova, S. Bakardjieva, and N. Murafa, "Photocatalytic activity of boron-modified titania under UV and visible-light illumination," *ACS Applied Materials and Interfaces*, vol. 2, no. 2, pp. 575–580, 2010.

[23] A. Weibel, R. Bouchet, F. Boulc'h, and P. Knauth, "The big problem of small particles: a comparison of methods for determination of particle size in nanocrystalline anatase powders," *Chemistry of Materials*, vol. 17, no. 9, pp. 2378–2385, 2005.

[24] B. I. Stefanov, Z. Topalian, C. G. Granqvist, and L. Österlund, "Acetaldehyde adsorption and condensation on anatase TiO_2: influence of acetaldehyde dimerization," *Journal of Molecular Catalysis A: Chemical*, vol. 381, pp. 77–88, 2014.

[25] X. Wang, M. Blackford, K. Prince, and R. A. Caruso, "Preparation of boron-doped porous titania networks containing gold nanoparticles with enhanced visible-light photocatalytic activity," *ACS Applied Materials and Interfaces*, vol. 4, no. 1, pp. 476–482, 2012.

[26] P. Carmichael, D. Hazafy, D. S. Bhachu, A. Mills, J. A. Darr, and I. P. Parkin, "Atmospheric pressure chemical vapour deposition of boron doped titanium dioxide for photocatalytic water reduction and oxidation," *Physical Chemistry Chemical Physics*, vol. 15, pp. 16788–16794, 2013.

[27] N. Feng, A. Zheng, Q. Wang et al., "Boron environments in B-doped and (B, N)-codoped TiO_2 photocatalysts: a combined solid-state NMR and theoretical calculation study," *Journal of Physical Chemistry C*, vol. 115, no. 6, pp. 2709–2719, 2011.

[28] A. Zaleska, J. W. Sobczak, E. Grabowska, and J. Hupka, "Preparation and photocatalytic activity of boron-modified TiO_2

under UV and visible light," *Applied Catalysis B: Environmental*, vol. 78, no. 1-2, pp. 92–100, 2008.

[29] C.-H. Wei, X.-H. Tang, J.-R. Liang, and S.-Y. Tan, "Preparation, characterization and photocatalytic activities of boron- and cerium-codoped TiO_2," *Journal of Environmental Sciences*, vol. 19, no. 1, pp. 90–96, 2007.

[30] C. Yu, J. C. Yu, W. Zhou, and K. Yang, "WO_3 coupled P-TiO_2 photocatalysts with mesoporous structure," *Catalysis Letters*, vol. 140, no. 3-4, pp. 172–183, 2010.

[31] N. Lu, X. Quan, J. Li, S. Chen, H. Yu, and G. Chen, "Fabrication of boron-doped TiO_2 nanotube array electrode and investigation of its photoelectrochemical capability," *The Journal of Physical Chemistry C*, vol. 111, no. 32, pp. 11836–11842, 2007.

[32] Y. Wu, M. Xing, and J. Zhang, "Gel-hydrothermal synthesis of carbon and boron co-doped TiO_2 and evaluating its photocatalytic activity," *Journal of Hazardous Materials*, vol. 192, no. 1, pp. 368–373, 2011.

[33] A. Zaleska, E. Grabowska, J. W. Sobczak, M. Gazda, and J. Hupka, "Photocatalytic activity of boron-modified TiO_2 under visible light: The effect of boron content, calcination temperature and TiO_2 matrix," *Applied Catalysis B Environmental*, vol. 89, no. 3-4, pp. 469–475, 2009.

[34] N. O. Gopal, H. Lo, and S. Ke, "Chemical state and environment of boron dopant in B,N-codoped anatase TiO_2 nanoparticles: an avenue for probing diamagnetic dopants in TiO_2 by electron paramagnetic resonance spectroscopy," *Journal of the American Chemical Society*, vol. 130, no. 9, pp. 2760–2761, 2008.